FORMATION OF THE LUNAR ATMOSPHERE*

R. R. HODGES, JR.
The University of Texas at Dallas, Richardson, Tex., U.S.A.

Abstract. Measurements of ^{40}Ar and helium made by the Apollo 17 lunar surface mass-spectrometer are used in the synthesis of atmospheric supply and loss mechanisms. The argon data indicate that about 8% of the ^{40}Ar produced in the Moon due to decay of ^{40}K is released to the atmosphere and subsequently lost. Variability of the atmospheric abundance of argon requires that the source be localized, probably in an unfractionated, partially molten core. If so, the radiogenic helium released with the argon amounts to 10% of the atmospheric helium supply. The total rate of helium escape from the Moon accounts for only 60% of the solar wind α particle influx. This seems to require a nonthermal escape mechanism for trapped solar-wind gases, probably involving weathering of exposed soil grain surfaces by solar wind protons.

1. Introduction

Gas pressure on the Moon is so low that there is essentially no meteorological influence either on lateral heat flow or orographic weathering. The main function of the lunar atmosphere is to act as a reservoir for temporary storage of free atoms and molecules, providing a pathway for escape of certain elements from the Moon. It also has acted over geologic time as a flow channel for lateral dispersal of volatile elements which have condensed on soil grain surfaces, and as a source of some of the ions which have been implanted in these grains.

The most significant aspect of the modern lunar atmosphere is its relationship to escape. Hydrogen and helium are lost from the Moon due to Jeans's classical mechanism of thermal evaporation. Heavier particles escape as ions which are formed mainly by photon impact and less frequently by charge exchange with solar wind protons. These ions are accelerated by the induced $\mathbf{v} \times \mathbf{B}$ force in the solar wind. Most escape the Moon, but some impact it and become implanted in soil grains. Manka and Michel (1971) suggest this mechanism to be responsible for the parentless ^{40}Ar found in returned soil samples.

The importance of the problem of atmospheric escape can be demonstrated by quoting some results which are subsequently discussed more fully in this paper. Specifically, the rate of escape of ^{40}Ar from the Moon appears to be variable, implying an episodic process of release of this radiogenic gas from the interior of the Moon. The average rate of loss of argon from the lunar atmosphere is about 2×10^{21} atoms s^{-1}, which is about 8% of the present argon production rate for the entire moon (2.4×10^{22} atoms s^{-1}) if the average lunar potassium abundance is about 100 ppm as suggested by Taylor and Jakeš (1974) and by Ganapathy and Anders (1974). To put these rates in planetologic perspective, the present rate of release of ^{40}Ar to the

* Paper presented at the Conference on 'Interactions of the Interplanetary Plasma with the Modern and Ancient Moon', sponsored by the Lunar Science Institute, Houston, Texas and held at the Lake Geneva Campus of George Williams College, Wisconsin, between September 30 and October 4, 1974.

The Moon **14** (1975) 139–157.

terrestrial atmosphere from one lunar mass of Earth is about 1.4×10^{22} atoms s^{-1} if the fraction of total production effusing into the atmosphere has remained constant over geologic time.

It is surprising that the rates of effusion of ^{40}Ar from the Moon and Earth are comparable when their atmospheric abundances differ by more than 15 orders of magnitude. The answer to this puzzle lies in differing escape processes. On Earth the escape of ions is inhibited by the geomagnetic field, so that almost all of the argon ever released is now present in the atmosphere. However, the lack of both a lunar magnetic field and an ionosphere allows the solar wind to impinge directly on the planet; and, hence, to accelerate any ions formed near the Moon. As a result, the average lifetime for lunar argon is only about 80 to 100 days. The product of lifetime and loss rate gives atmospheric abundance, which amounts to the minuscule lunar atmosphere having about 10^6 gm of argon.

In essence, the lunar atmosphere serves as a pipeline for escape, not only of argon, but of virtually all atmospheric gases. Viewed in another way, the atmospheric abundance of a gas specifies its escape rate, which in turn specifies a loss parameter for the entire Moon. The importance of the argon loss is obvious in modeling the lunar interior. Another example is that only 60% of the solar wind influx of helium is currently escaping from the lunar atmosphere, which implies the existence of a second, nonthermal loss mechanism for helium and, hence, for other solar wind gases as well.

The key to understanding present lunar atmospheric escape, and the past influence of the atmosphere on the distribution of volatile elements in the regolith as well, lies in the tedious process of atmospheric modeling. Collisions between particles are so infrequent that the lunar atmosphere is usually considered to be entirely an exosphere, with the regolith serving as a classical exobase. Atoms and molecules travel in ballistic trajectories between encounters with the regolith. Upgoing velocities at the surface have thermal distribution, resulting in the average lateral extent of a trajectory being proportional to temperature and inversely proportional to mass. The light gases, hydrogen and helium, have significant fractions of hyperbolic orbits to account for most of their escape rates, whereas this thermal evaporation is virtually nonexistent for heavier species.

Owing to the temperature dependence of the average lateral extent of ballistic trajectories a particle moves down a temperature gradient in larger steps than it moves up. In the absence of surface adsorption this results in a statistical preference of an exospheric particle to spend more time in the cold nighttime region than in daytime. The cumulative statistical effect of many atoms is a nighttime concentration maximum. Hodges and Johnson (1968) have shown that ballistic transport causes an exospheric lateral flow pattern which approximately tends to equalize $nT^{5/2}$ over the exobase (where n is concentration and T is temperature.) Thus, the nearly 4 to 1 day to night surface temperature ratio on the Moon should result in about a 30 to 1 night to day ratio of concentration. This condition is nearly attained by helium, but many other gases seem to be adsorbed at night, creating a nighttime minimum and a maximum at sunrise where desorption tends to occur.

Surface processes of adsorption and desorption are species dependent as well as being functions of temperature and solar illumination (for desorption). As a result it is necessary to synthesize these parameters from experimental data. The only extensive, artifact-free data on condensible gas are the Apollo 17 mass spectrometer measurements of ^{40}Ar. Some limited data, reported in a separate paper by Hoffman and Hodges (1975), show qualitative evidence for the existence of other condensible gases on the Moon.

To pursue the subject of the formation of the lunar atmosphere it is necessary to be specific regarding species. Therefore, subsequent discussion will concentrate on the two best understood lunar gases: ^{40}Ar and helium. It is fortunate that these represent extremes of lunar atmospheric physics. The argon is radiogenic and entirely of lunar origin, reflecting the degassing of the interior of the Moon. In contrast most of the helium comes from solar wind α particles which have impacted the Moon. Another important difference is that argon is adsorbed at night while helium is not. In addition the sticking time of argon is short enough that desorption has a noticeable effect at night. Following the sections on argon and helium is a less quantitative discussion of other atmospheric processes and constituents.

In subsequent analysis all atmospheric modeling is based on a Monte Carlo technique which was first reported in Hodges (1973) and modified as noted in Hodges *et al.* (1974) and Hodges (1974). Briefly, the modeling technique simulates the lunar atmosphere by following the trajectories of a succession of individual molecules over the surface of the Moon, from creation to annihilation. Global variations of statistical parameters, such as the effects of temperature on the velocity distribution of atoms following surface encounters, and probabilities of adsorption, desorption, creation, and photoionization are taken into account. Particle lifetime is found by accumulating total time of flight and of adsorption. The influence of the perturbation of the lunar gravitational potential by the Earth is approximated by assuming that particles with greater energy than is required to reach the inner Lagrangian collinear point (0.956 times lunar escape energy; cf. Kopal, 1966) are lost from the Moon. This seemingly slight difference in the definition of escape has the surprisingly large effect of halving the average lifetime of helium atoms.

2. ^{40}Ar

The ^{40}Ar data from the Apollo 17 lunar surface mass spectrometer have been presented in Hodges and Hoffman (1974a). Figure 1 shows the entire data set available from that experiment, which consists of lunar nightime measurements through the first 9 lunations of 1973. Daytime measurements were precluded by high rates of degassing of remnant spaceflight hardware in sunlight.

Figure 2 shows the nature of the synodic variation of argon by superposition of data from the two lunations in which the maximum and minimum abundances of argon occurred. It is immediately apparent that the amount of argon on the Moon dropped by about a factor of 2 in a four month period. The history of the 1973 argon variation and its implications are discussed later.

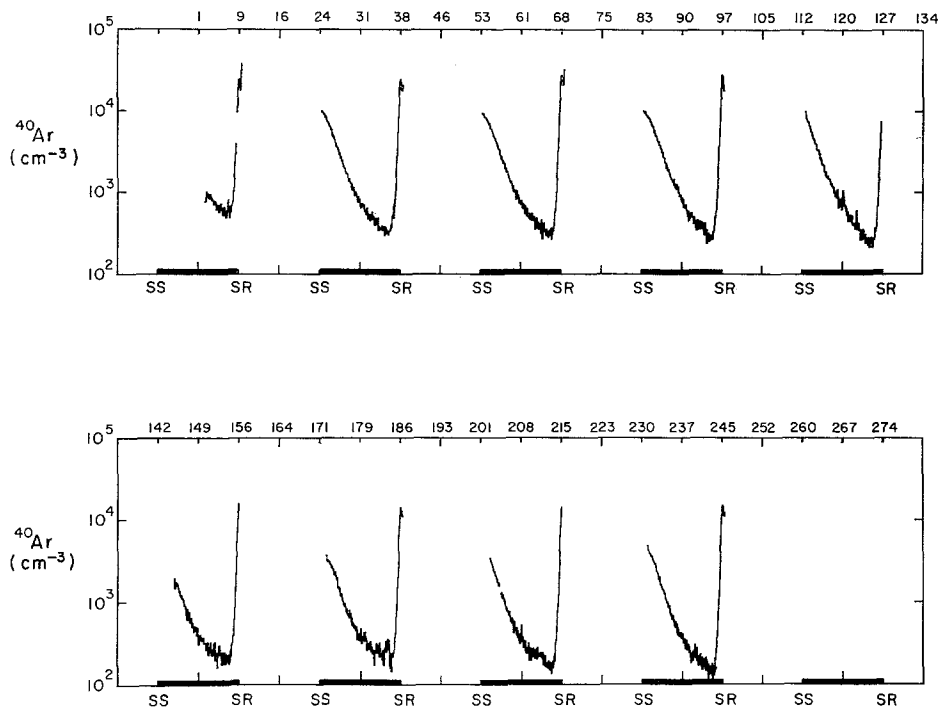

Fig. 1. Measured concentration of ^{40}Ar at the Apollo 17 site during 1973. The upper abscissa gives calendar days of quarterphases of the Sun. Sunrises (SR), sunsets (SS), and periods of darkness (dark bar) are specified on the lower scale.

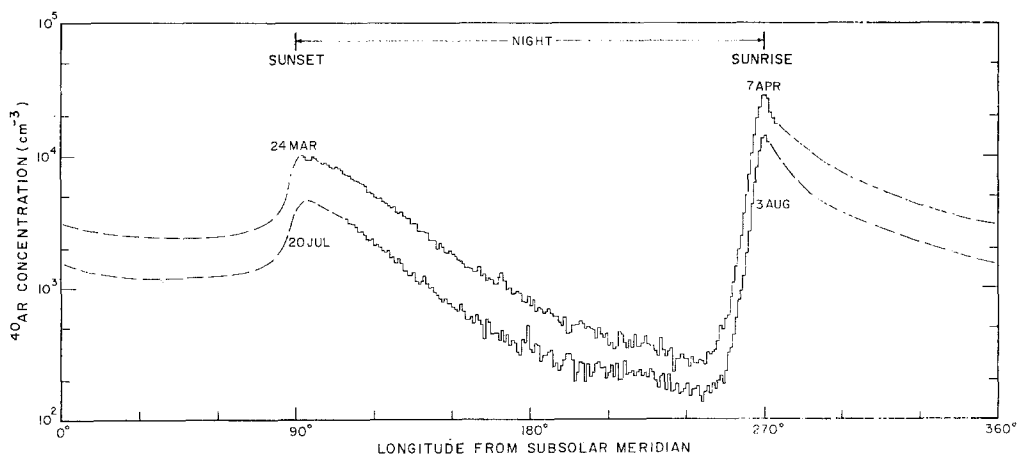

Fig. 2. Synodic variations of ^{40}Ar during lunations of maximum and minimum abundances. Dashed curves are theoretical extrapolations which show expected daytime behavior.

The synodic variation of argon is characteristic of a condensible gas. The slow post sunset decrease in concentration indicates an increasing adsorption probability with decreasing temperature, while the nearly asymptotic behavior of the nighttime minimum requires an appreciable amount of desorption. At sunrise the bulk of the adsorbed gas is released from the lunar surface, and some of it travels into the nighttime hemisphere, giving rise to the rapid presunrise increase. Incidentally, it is the presunrise buildup which marks this data as an actual indication of a lunar gas; there is no apparent way for an artifact release to anticipate sunrise in this manner.

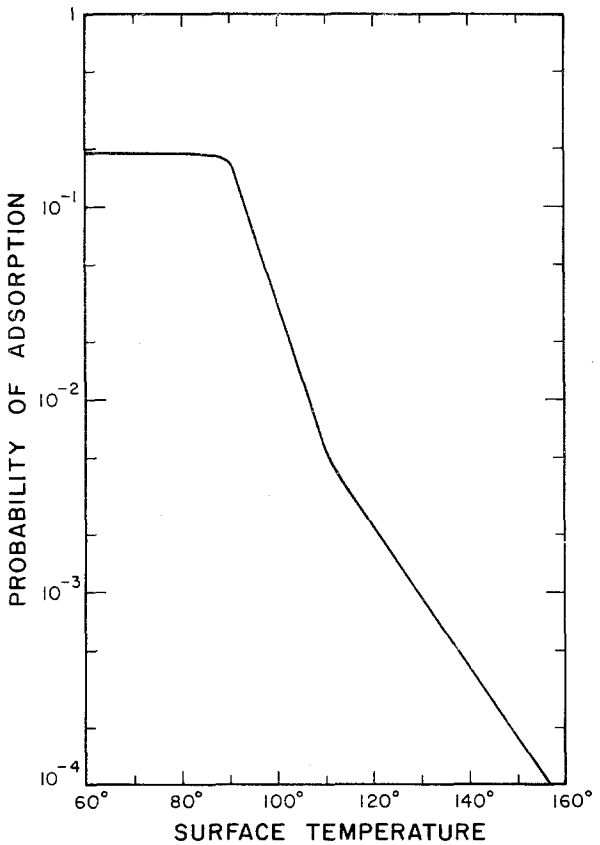

Fig. 3. Probability of adsorption of atmospheric argon on the lunar surface as a function of temperature.

A series of Monte Carlo simulated argon atmospheres were calculated, in which adsorption and desorption dependencies on temperature and solar illumination were iteratively adjusted until the synodic variation at 20° latitude of the model distribution matched the average measured variation. The best fit of model and experiment seems to occur for the adsorption probability function shown in Figure 3. Two forms of desorption are needed to explain the data. The first is the spontaneous process of thermal desorption, which apparently depends on temperature in a manner similar to

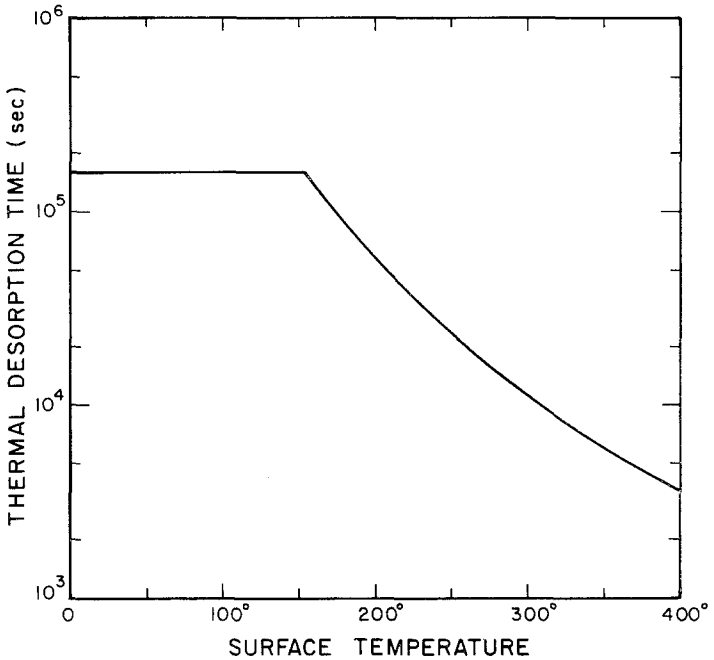

Fig. 4. Mean thermal desorption time for argon on the lunar surface as a function of temperature.

the graph of Figure 4. (The break in the curve near 150 K is an artifact introduced for analytical simplicity.) The second desorption mechanism is a photon process in which qualitative laboratory tests show that certain gases, including argon, are released from a surface by the visible range of the solar spectrum. In order that the model reproduce the measured sunrise to sunset concentration ratio it is necessary that the illumination of a soil grain surface release an atom with unity probability. To account for soil texture and orography it is assumed that the probability of illumination of an exposed soil surface increases from 0 to 0.5 as lunar rotation moves the grain through a band of $\pm 2°$ of solar zenith angle about the spherical moon sunrise terminator, and that the probability of illumination of the remaining surface area increases linearly thereafter with increasing zenith angle. In practice about half of the atoms adsorbed at low latitude are released by the photon interaction process, while spontaneous desorption is more likely at high latitudes where the time needed for sunrise to traverse the orographic uncertainty becomes quite long.

The adsorption and desorption characteristics discussed above are the result of synthesis; and, hence, are not unique answers to the problem. However, the sensitivity of model atmospheres to small changes in these parameters suggests that the present results are likely to closely approximate the true lunar conditions. One nagging question is that the soil near the Apollo 17 site may not reflect average lunar characteristics. A possible way to proceed with this problem would be to construct a gas chromatographic column with lunar soil from various Apollo landing sites used as the buffer material to make direct measurements of adsorption and desorption characteristics.

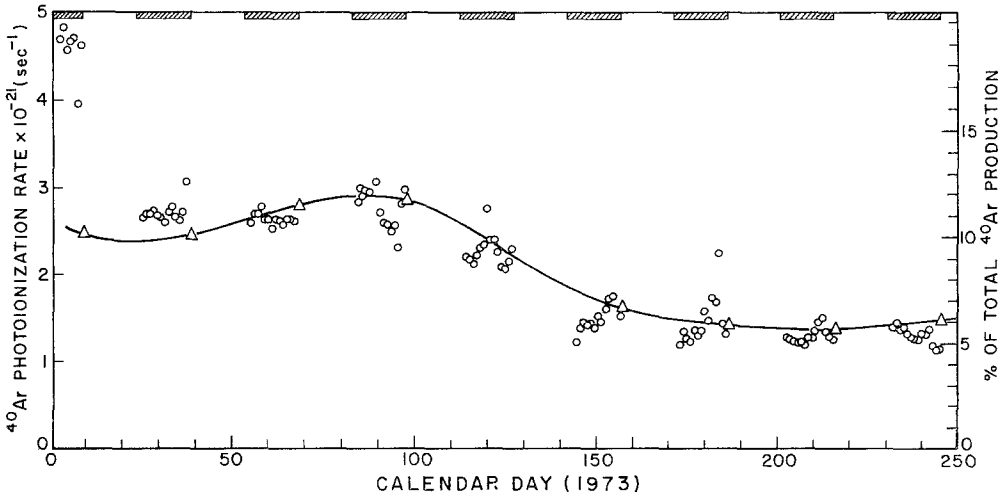

Fig. 5. Temporal variation in the rate of photoionization of ^{40}Ar in the lunar atmosphere during 1973. Triangles give sunrise values, while circles represent less accurate rates inferred from nighttime measurements.

Among the parameters to emerge from the model study are the following. Average argon lifetime on the Moon is about 100 days, of which 80% of the time is spent adsorbed on the surface. The average sticking time for an adsorbed atom is 1.1 days. The rate of photoionization of argon in the lunar atmosphere (number of atoms per second) is about 9×10^{16} times the sunrise concentration at the Apollo 17 latitude (20°). Thus the loss rate corresponding to the average argon sunrise concentration ($\sim 2 \times 10^4$ cm^{-3}) is about 2×10^{21} atoms s^{-1}.

Figure 5 shows the temporal variation of the total argon photoionization rate during 1973. It should be noted that this rate is proportional to both atmospheric abundance and to escape rate. Triangles represent the most accurate determinations of the photoionization rate at sunrises where the concentration is greatest. Each circle gives the rate found by model extrapolation of a 5° longitudinal average of concentration to an equivalent sunrise concentration. High values of the circles early in the year are due to a decaying artifact contribution to the low nighttime concentration. The large variance of the photoionization rate represented by the circles is indicative of the noise inherent in the nighttime concentration data and errors in the model.

As mentioned earlier there are two important aspects of the ^{40}Ar photoionization rate, which show up clearly in Figure 5. First, the time average of the rate is roughly 2×10^{21} atoms s^{-1}, corresponding to about 8% of the total lunar production of ^{40}Ar if the potassium abundance is 100 ppm. If a large fraction of the photoions were to impact the lunar surface and subsequently become recycled into the atmosphere, then the actual source of new atoms would be a lesser part of the production rate. However, the second obvious feature of Figure 5, the time variation of the photoionization rate (and hence of argon abundance), argues strongly that there is very little recycling of ^{40}Ar.

The clue that argon recycling is unimportant is found in the decay of the photoionization rate between about day 100 and day 150, where the decay time constant is roughly equivalent to the average lifetime of argon atoms – i.e., about 100 days. If ψ_0 is used to denote the total supply of atoms, both new and recycled, to the atmosphere, and ψ_i is the photoionization rate, then continuity requires that

$$\psi_s = \psi_i + \tau \frac{d\psi_i}{dt}, \tag{1}$$

where τ is the average atomic lifetime. Figure 6 shows the aron source, ψ_s, required to supply the photoionization rate shown in Figure 5 for three values of the lifetime τ.

An important feature of Equation (1), and hence of Figure 6, is that the total argon source must include an essentially constant contribution from recycled atoms, and that temporal variation of ψ_s must arise from internal changes in the Moon which affect the rate of release of new argon atoms. Since ψ_s is a positive definite quantity, it is obvious that the lifetime which emerges from the atmospheric model calculations, 100 days, is nearly an upper bound. In addition, the 100-day lifetime allows for very little recycled argon. A decrease in the lifetime to 60 days would be consistent with a

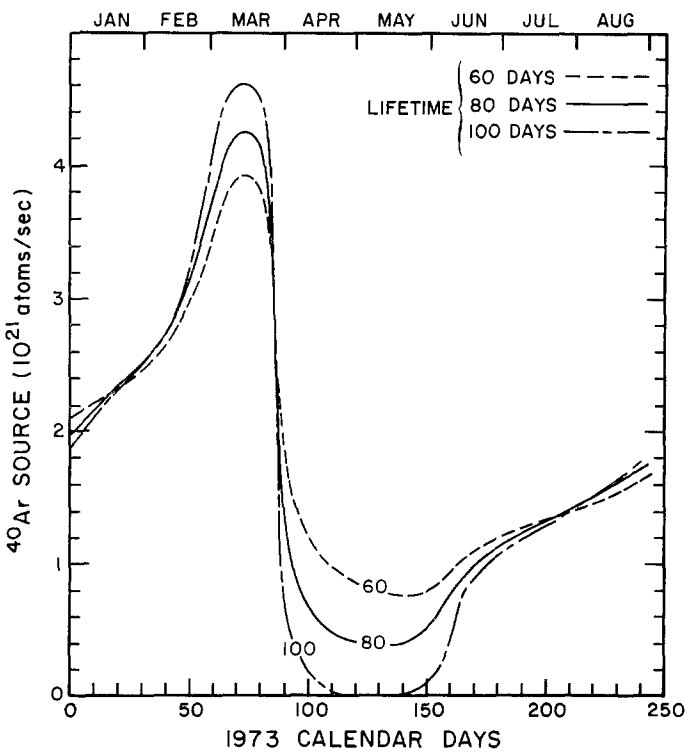

Fig. 6. The total source of ^{40}Ar needed to explain the measured atmospheric argon during 1973 for several values of the mean atomic lifetime.

recycling rate of about 8×10^{20} atoms s^{-1} or roughly 40% of the total source. However, model calculations for a wide variety of surface parameters have consistently given a lifetime in excess of 80 days. The shortest model lifetimes occur when adsorption probability is increased near the poles, but this always produces an inconsistently large sunset concentration at the Apollo 17 latitude (20°). Thus the best judgment is that the recycling fraction of the total argon photoionization rate is quite small, and that it probably is less than 10% to be consistent with a lifetime in the 80–100 day range. This places some constraints on the rate of release of retrapped, parentless ^{40}Ar from the regolith.

The most puzzling aspects of the ^{40}Ar source are its large average amplitude and its episodic nature. To put the average release rate in perspective, the release of 2×10^{21} atoms s^{-1} would correspond to release of each argon atom as it is created in the upper 8 km of the Moon if the average crustal potassium abundance is the highlands average of 600 ppm suggested by Taylor and Jakeš (1974). However, the release of these atoms

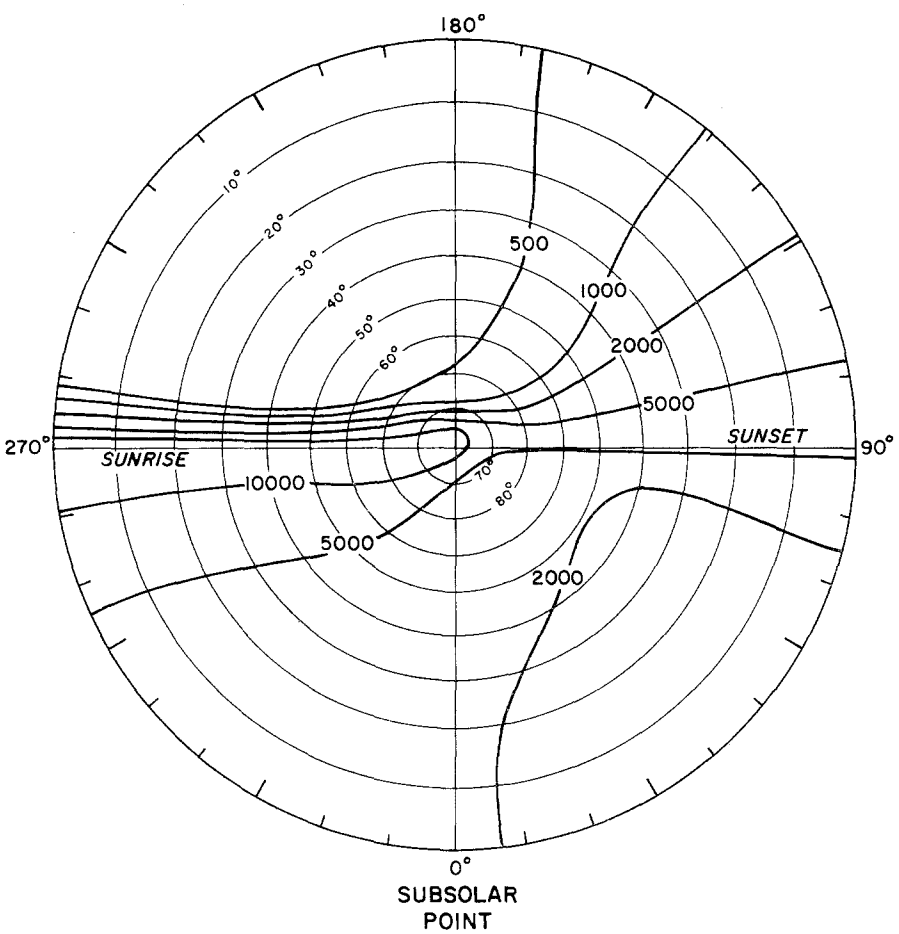

Fig. 7. The hemispheric distribution of ^{40}Ar on the lunar surface.

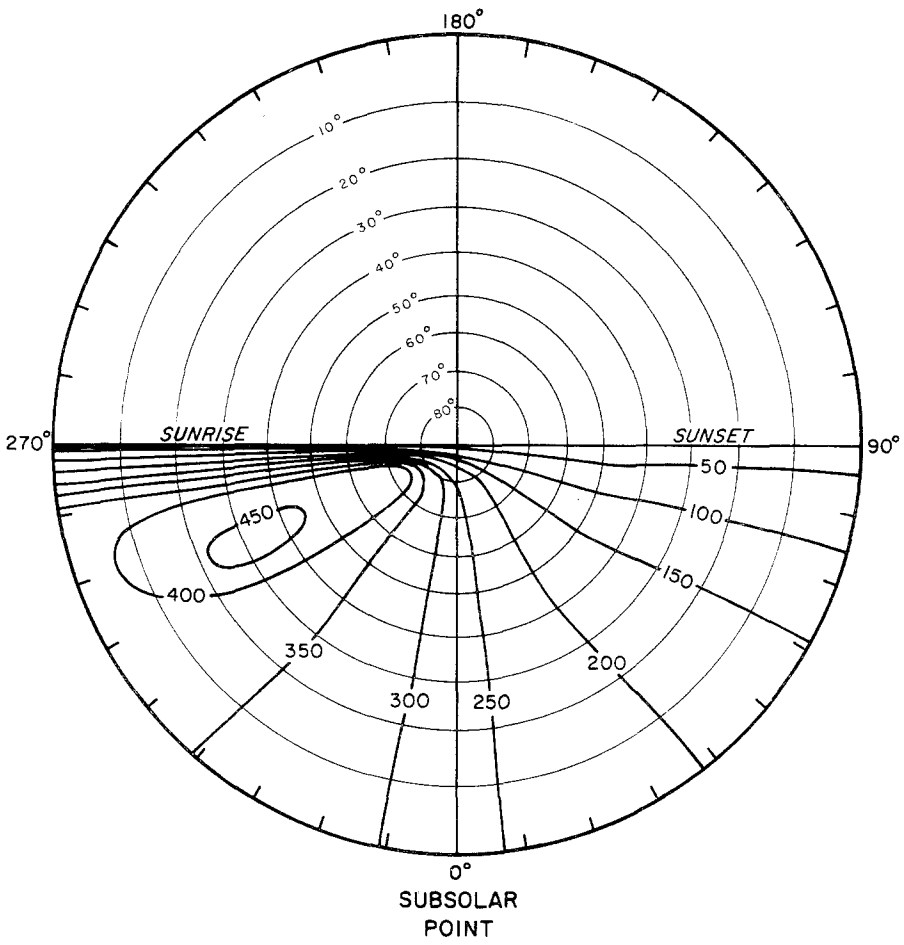

Fig. 8. The hemispheric distribution of ^{40}Ar at an altitude of 100 km above the lunar surface.

is incompatible with known weathering mechanisms. This requires consideration of a deeper source region. If the argon were postulated to come from greater depths where radioactive heating enhances diffusion of the argon atoms out of rocks and into fractured areas, the time variation would still be difficult to explain.

The only remaining source of the atmospheric argon is a semi-molten core with radius of about 750 km if the potassium abundance there is 100 ppm. This size fortuitously corresponds to one of the models proposed by Taylor and Jakeš (1974), in which a partially molten zone of primitive unfractionated lunar material occupies a core of about 750 km radius. It is also consistent with analyses of seismic data which suggest partial melting in this region (Latham *et al.*, 1973). The problem of explaining the time variation remains. Hodges and Hoffman (1974a) have suggested that there may be a correlation with seismic processes, and that either the release of argon is due to internal movements which periodically open paths to the lunar surface, or the

pressure of gas trapped in voids of the core periodically builds up to a point where the gas opens its own vent to the surface, possibly creating a seismic signal.

The rate of release of lunar radiogenic argon is so strongly tied to the interior structure of the Moon that long term measurements of atmospheric argon must eventually be made. Interpretation of such measurements will involve extrapolation of total abundance from local data. Figure 7 shows the presently most realistic model of the distribution of ^{40}Ar at the lunar surface as a topographic map in sterographic projection of the northern hemisphere. It can be noted that the sunrise and sunset maxima extend to the polar region. What is, unfortunately, not practical to show is that the maximum concentration occurs in the polar region, and is about 4×10^4 atoms cc^{-1}, or about twice the equatorial sunrise level.

Figure 8 shows the distribution of ^{40}Ar expected to be encountered by an orbiter at 100 km altitude. At night the concentration becomes too small to measure, but experience with the Apollo 17 lunar surface mass spectrometer suggests that the daytime concentrations above 50 atoms cc^{-1} could be measured by a mass spectrograph dedicated to integration of the argon peak, and designed to operate with a cold inlet system (<270 K) to suppress artifact background gases.

3. Helium

The sources of helium in the lunar atmosphere are the α particles supplied by solar wind implantation in the regolith and by decay of ^{232}Th and ^{238}U within the Moon. Johnson *et al.* (1972) have reviewed the available solar wind data and concluded that the average α particle flux is about 1.35×10^7 cm^{-2} s^{-1}, corresponding to 4.5% of the proton flux. This should result in a helium supply of 1.3×10^{24} atoms s^{-1} on the Moon. The rate of production of radiogenic helium in the Moon can be estimated by assuming the bulk Moon abundance of Th to be 0.23 ppm and U to be 0.06 ppm (cf. Taylor and Jakeš, 1974). Decay of these elements to stable lead results in a total helium source of 1.2×10^{24} atoms s^{-1}. If K, U and Th distributions in the Moon are similar then the mechanism for release of helium should be the same as that of ^{40}Ar, and, hence, the rate of supply of radiogenic helium to the lunar atmosphere should be about 10^{23} atoms s^{-1}. Thus the total available source of lunar atmospheric helium is about 1.4×10^{24} atoms s^{-1}.

Figure 9 shows theoretical and average experimental data on the synodic variation of helium at the Apollo 17 site (20° latitude). The solid line represents a numerically smoothed model obtained from a Monte Carlo calculation in which 180 impact zones were distributed longitudinally in the 20° latitude region. Amplitude of the model distribution is based on a source equivalent to the average solar wind influx of 1.3×10^{24} atoms s^{-1}.

The experimental data points in Figure 9 are from Hodges and Hoffman (1974b). Each point corresponds to an average of all available measurements which occurred during the first 10 lunations of 1973) in an 18° increment of longitude. Error bars represent the variances of these blocks of data, but they indicate systematic temporal

changes in helium abundance rather than a useful parameter of the statistical distribution of the data. The measurements were confined to lunar nighttime because of instrument operational constraints, but they suggest a good correspondence of the actual atmosphere with the theoretical model.

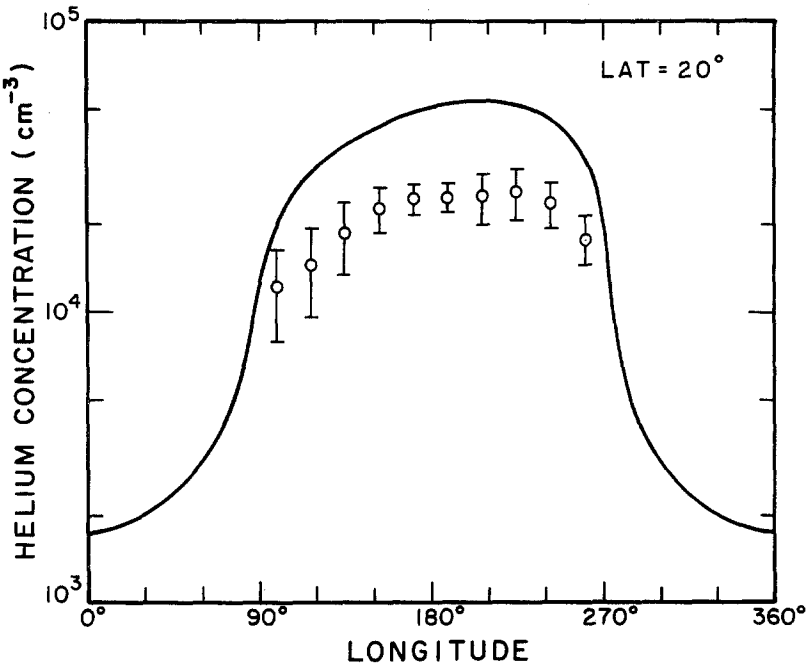

Fig. 9. Synodic variation of helium on the Moon. The solid line gives the model distribution for a solar wind source of 1.35×10^7 α particles cm^{-2} s^{-1}. Data points represent averages of all Apollo 17 mass spectrometer measurements in 18° bands of longitude.

In Figure 9 it is evident that the actual helium abundance is only about 70% of the model value and, hence, the average helium source in 1973 was probably about 9×10^{23} atoms s^{-1}. Subtracting the radiogenic source, the solar wind must have supplied about 8×10^{23} atoms s^{-1}, or about 60% of the average solar wind α particle influx. An explanation of the apparently low atmospheric supply rate is presented later.

A detailed history of the helium data, shown in Figure 10, reveals numerous deviations from the smooth model of the synodic variation. In these graphs the data has been subjected to 3 hr averaging, corresponding roughly to the atmospheric equilibration time, so that the ratio of the measured concentration to the model value at the same longitude is proportional to total atmospheric abundance at any time. The obvious deviations from the model distribution could only have occurred as responses of the atmosphere to sudden increases in the total amount of helium on the Moon. Their amplitudes appear to be too great to be accounted for by variations in the rate of effusion of radiogenic helium from the interior of the Moon.

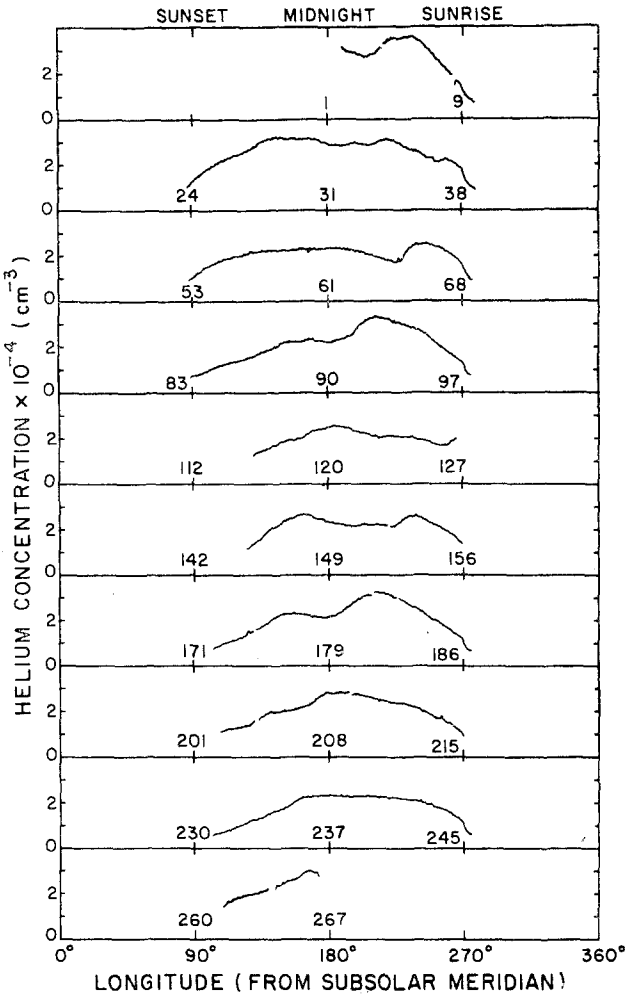

Fig. 10. Measured helium concentrations in the first 10 lunations of 1973.

The analysis of Hodges and Hoffman (1974b) showed a correlation of the variability of lunar atmospheric helium with the geomagnetic index Kp, and hence with the solar wind. This analysis was based on the equation of continuity

$$\phi_s = \phi_0 \left\{ \frac{n}{n_0} + \tau \frac{\mathrm{d}}{\mathrm{d}t} \left(\frac{n}{n_0} \right) \right\}, \tag{2}$$

where ϕ_s is the equivalent solar wind source flux of α particles necessary to supply atmospheric escape; ϕ_0, the flux used in the model calculation (1.35×10^7 cm^{-2} s^{-1}); n, the three hour average of the measured concentration; n_0, model concentration at the corresponding longitude; and τ is the average atomic lifetime for helium on the Moon. Note that the instantaneous escape rate is $\phi_0 n/n_0$.

Recent improvements in the Monte Carlo atmospheric modeling technique have included direct calculation of atomic lifetimes by summing the times of flight for all trajectories. This has resulted in a longer lifetime for helium than 8×10^4 s calculated in Hodges (1973) where lifetime was inferred from a barometric estimation of total helium abundance. The newly calculated lifetime is 2×10^5 s.

Figure 11 shows the correlation of ϕ_s, the equivalent solar wind α particle flux, with the geomagnetic index Kp for the 2×10^5 s lifetime. Circles represent average flux values in each increment of Kp, while error bars give the standard deviation of these fluxes. The upper graph gives the number of hours of data available at each value of Kp. Individual flux values are plotted for the infrequent condition $Kp > 6^+$.

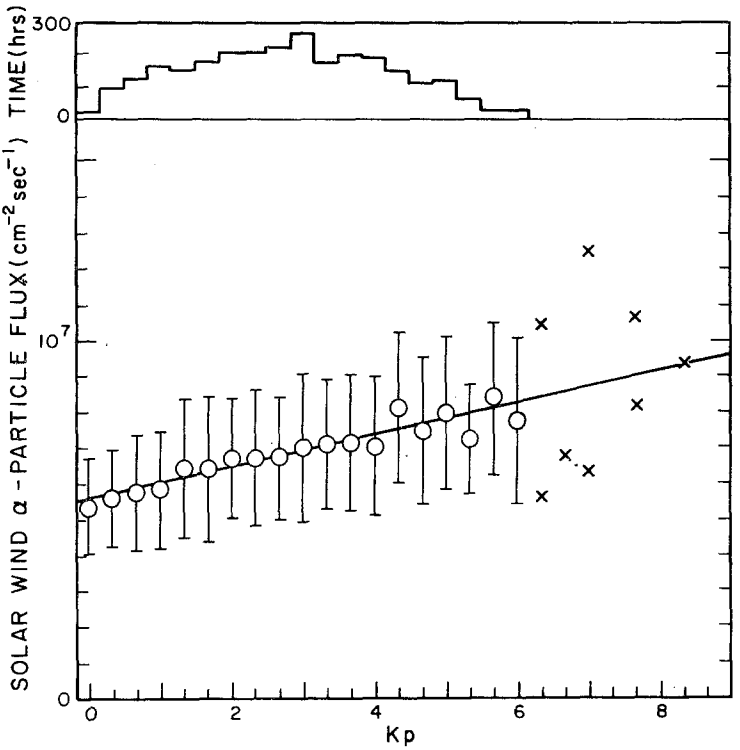

Fig. 11. The equivalent solar wind flux of helium needed to supply lunar atmospheric escape (lower graph) and total data accumulation time (upper graph) as functions of Kp. The straight line shows the linear regression of all of the data.

The straight line shown in Figure 11 gives the linear mean-square regression of all of the flux vs. Kp data. It shows that the equivalent solar wind α particle flux needed to supply the lunar atmosphere has the approximate relationship

$$\phi_s = (5.6 \pm 1.9 + 0.44 \times \mathrm{Kp}) \times 10^6 \ \mathrm{cm}^{-2} \ \mathrm{s}^{-1}. \tag{3}$$

This expression, and Figure 11 as well, differ from the results presented in Hodges

and Hoffman (1974b) because of the improved value of average lifetime used here.

The slope of the regression line in Figure 11 is not as steep as might be expected from the data on Kp correlations with the solar wind reported by Wilcox *et al.* (1967) and the results of Hirshberg *et al.* (1972). However, the apparent relationship of the equivalent lunar atmospheric source flux data and Kp has been numerically confirmed to have a correlation coefficient of 0.31. Therefore, it can be concluded that while the lunar atmosphere may depend on several helium source mechanisms, one of these is clearly related to Kp and hence to the solar wind. Since α particles impact the Moon with energies of about 4 keV, the solar wind mechanism probably does not involve the immediate neutralization of impacting α particles, but rather a process of release of previously trapped solar wind helium from soil grains.

Presumably the average rate of accretion of α particles by the lunar regolith nearly equals the average rate of release of previously trapped helium from the soil, with the slight unbalance due to the absorption of helium by previously unexposed material which has recently been brought to the lunar surface by meteor impacts. Diffusion must account for part of the release of trapped helium from the soil, but the solar wind related component is probably of greater importance.

A weathering process due to the solar wind could account for the solar wind correlated part of the helium source. One possibility is that the proton influx causes sputtering of soil grain surface material, resulting in volatilization of many elements, including trapped helium. This mechanism has been proposed by Housley (1974) as an important means of both lateral transport and escape. The fact that the present data seem to show a deficit of atmospheric helium, based on the average solar wind source, suggests that some helium is lost from the Moon as sputtered ions or as superthermal atoms which would not have been detected by the Apollo 17 mass spectrometer because its field of view was limited to nonescaping, downcoming atoms. The low energy fraction of sputtered helium could be the solar wind correlated source of lunar atmosphere.

If the hypothesis of release of trapped solar wind helium from the lunar soil by sputtering is correct, then the α particle fraction of the solar wind is not related to the unexpectedly low helium abundance in the lunar atmosphere in the 1973 measurements. The sputtered helium effusion rate must represent a very long term average of the solar wind helium implantation rate, modulated by variations in the weathering agent: the instantaneous influx of solar wind momentum.

In summary it appears that the average rate of escape of helium from the thermalized lunar atmosphere is about 9×10^{23} atoms s^{-1}, of which 10% is probably supplied by radioactive decay of Th and U in the Moon. The remaining atmospheric helium escape amounts to 60% of the solar wind inflow of α particles. The correlation of atmospheric helium with the geomagnetic index Kp suggests solar wind weathering of the soil to be an important mechanism for release of previously implanted solar wind helium. A superthermal or ionized component of the helium released by the surface weathering process seems to be needed to account for escape of the 40% of the solar wind helium which does not participate in the formation of the lunar atmosphere.

4. Other Atmospheric Processes

The foregoing atmospheric results have important implications on the physics of other volatiles on the Moon. For example, the measurements made by the Apollo 15 and 16 orbital α-particle spectrometers indicate the emanation of radon from the lunar interior to the atmosphere, a process which must be related to the release of ^{40}Ar.

What is important in the α-particle data is the rate of decay of ^{210}Po at the lunar surface, because this gives an average for the rate of diffusion of the gaseous progenator of the polonium, ^{222}Rn, to the surface region of the regolith over the last several decades. From the data reported by Bjorkholm *et al.* (1973) it appears that the average rate of ^{210}Po decay is in the range of 0.018 ± 0.01 dis cm^{-2} s^{-1}, which translates to a global average effusion rate for radon of about $7 \pm 4 \times 10^{15}$ atoms s^{-1}.

If we assume the bulk Moon average abundance of uranium to be 0.06 ppm as suggested by Taylor and Jakeš (1974), the total lunar rate of production of ^{222}Rn is 8×10^{22} atoms s^{-1}. If the radon and ^{40}Ar source regions are the same, then about 8% of the radon or 6×10^{21} atoms/sec are available for transport to the lunar surface. Owing to the 3.8 day half life of radon, the large difference between the available supply and the surface effusion rate implies an average transit time of 70 to 80 days.

The argument for correlation of the argon and radon source regions suggests further preference for the model of the lunar interior proposed by Taylor and Jakeš (1974) in which the Moon has an unfractionated, partially molten core with radius of about 750 km, in which K and U are present in roughly their bulk Moon average abundances. Surface measurements of argon and radon are compatible with a release process in which radiogenic gases collect in bubble-like regions of the core. The collecting gases are vented to the lunar surface whenever the pressure reaches some critical level. To maintain the measured ^{210}Po level at the lunar surface the storage time for these pockets of gas must be on the order of 80 days, but the paucity of both argon and radon data allows for a large deviation of this time and of its average value.

Gorenstein *et al.* (1973) report spatial variations in the distribution of ^{210}Po on the Moon, which indicate localized emissions of radon followed by limited atmospheric transport prior to decay to polonium. Localized venting is in agreement with the idea of transient release of radiogenic ^{40}Ar and radon from the lunar core. However, Gorenstein *et al.* go on to suggest an episodic variability of the rate of radon emanation on a time scale of 10 to 60 yr to explain present excesses of polonium over radon on some regions of the lunar surface. This would suggest an implausible change in venting of the gas from the core over a geologically short time. One possible way out of this dilemma is to postulate that the excess part of the polonium now decaying on the lunar surface has been brought there by upward transport through the soil, perhaps via the mechanism of electrostatic levitation of dust, a process which has been discussed as the cause of horizon glow in post sunset Surveyor 7 photography by Criswell (1972). The influence of orography on the production of electric fields at the lunar surface is a possible cause of spatial differences in electrostatic regolith overturning and, hence, in the rate of migration of polonium to the surface.

The apparent evidence for regolith weathering in the present interpretation of the Apollo 17 mass spectrometric helium measurements implies that the sputtering process must affect other elements as well. This mechanism has been discussed by Housley (1974); its quantitative influence on expected lunar atmospheric gases is presented here.

Attempts at detection of the solar wind gases in the lunar atmosphere have generally been unproductive. Fastie *et al.* (1973) give an upper bound on H which is orders of magnitude below model abundances calculated by Hartle and Thomas (1974) and by Hodges *et al.* (1974). The later authors also report tentative interpretations of ^{20}Ne and ^{36}Ar measurements, which may also be considered to be upper bounds.

The pre-sunrise mass spectrometer data discussed by Hoffman and Hodges (1975) shows evidence of only slight amounts of some gases which are copiously supplied by the solar wind. Of particular interest is methane, which has about 2% the sunrise concentration of ^{40}Ar, despite a solar wind influx of carbon that is nearly 2 orders of magnitude greater than the average ^{40}Ar source. It is tempting to ascribe the atmospheric deficit of carbon to continuing implantation of solar wind ions in the soil. However, there are some serious problems with this argument. At the Apollo landing sites, where the lunar surface is shielded from the solar wind about 4 days per lunation by the geomagnetic tail, the net carbon influx is roughly 10^{13} ion cm^{-2} s^{-1}. If the soil has been steadily assimilating this carbon, then the present surface abundance of about 100 ppm translates to a mixing scale depth of 10 m b.y.$^{-1}$. However, the intensity of turbulence produced by meteor impacts must diminish with increasing depth, making uniform mixing implausible, and hence forcing the needed depth of mixing far beyond 10 m b.y.$^{-1}$. In contrast, the neutron capture data of Burnett and Woolum (1974) suggests that in the last 0.5 b.y.$^{-1}$ soil accretion rather than mixing of the regolith has occurred at the sites of the Apollo 15 and 16 deep core samples. The lack of an adequate global soil mixing mechanism indicates that an important fraction of the solar wind carbon must escape from the Moon. Thus the low levels of methane and other carbon gases in the atmosphere are difficult to explain.

Attempts to devise adsorption and desorption parameters for a methane atmospheric model which has a low terminator concentration at the Apollo 17 latitude have not been fruitful. The problem is a need for a large amount of the gas in sunlight if photoionization is the dominant cause of loss. It is possible that the adsorption probability for methane approaches unity at high latitudes, even in daytime, leading to the formation of a localized surface monolayer of methane in each polar region. Desorption from these deposits could supply virtually all photoionization losses of methane while precluding atmospheric formation at low latitudes.

Proof of the feasibility of the above model depends on further attempts at modeling. The alternative is that almost all of the solar wind carbon implanted in the soil eventually escapes due to sputtering. This seems to be contrary to the helium data discussed above, since at most only about 40% of the solar wind α particle influx is not accounted for by atmospheric escape. In addition the noticeable changes in atmospheric helium due to solar wind fluctuations suggest that an important fraction of the

helium released by proton impact has thermal energy. Thus, the nonthermal escape of a large fraction of trapped solar wind carbon from the regolith would require a mechanism which imparts orders of magnitude more kinetic energy to carbon than to helium. In a word, the escape of solar wind elements other than helium remains an enigma.

5. Conclusions

The dominant gases of the lunar atmosphere seem to be ^{40}Ar and helium. Owing to a lack of atomic collisions, each gas forms an independent atmospheric distribution. Argon is adsorbed on lunar surface soil grains at night, causing a nighttime concentration minimum. In contrast helium is virtually noncondensible, and hence has a nighttime maximum of concentration in accordance with the classical law of exospheric equilibrium.

Essentially all of the ^{40}Ar on the Moon comes from the decay of ^{40}K in the lunar interior. Variability of the amount of atmospheric argon suggests a localized source region. The magnitude of the average escape rate, about 8% of the total lunar argon production rate, indicates that the source may be a partially molten core with radius of about 750 km, from which all argon is released.

Most of the helium in the lunar atmosphere is of solar wind origin, although about 10% may be due to effusion of radiogenic helium from the lunar interior. The atmospheric helium abundance changes in response to solar wind fluctuations, suggesting surface weathering by the solar wind as a release mechanism for trapped helium. Atmospheric escape accounts for the radiogenic helium and about 60% of the solar wind α particle influx. The mode of loss of the remaining solar wind helium is probably nonthermal sputtering from soil grain surfaces.

Acknowledgment

This research was supported by NASA Grant NSG-7034.

References

Bjorkholm, P. J., Golub, L., and Gorenstein, P.: 1973, *Proc. Fourth Lunar Science Conf., Geochim. Cosmochim. Acta, Suppl. 4*, **3**, 2793–2802.

Burnett, D. S. and Woolum, D. S.: 1974, *Proc. Fifth Lunar Science Conf., Geochim. Cosmochim. Acta, Suppl. 5*, **2**, 2061–2074.

Criswell, D. R.: 1972, *Proc. Third Lunar Science Conf., Geochim. Cosmochim. Acta, Suppl. 3*, **3**, 2671–2680.

Fastie, W. G., Feldman, P. D., Henry, R. C., Moos, H. W., Barth, C. A., Thomas, G. E., and Donahue, T. M.: 1973, *Science* **182**, 710–711.

Ganapathy, R. and Anders, E.: 1974, *Proc. Fifth Lunar Science Conf., Geochim. Cosmochim. Acta, Suppl. 5*, **2**, 1181-1206.

Gorenstein, P., Golub, L., and Bjorkholm, P. J.: 1973, *Proc. Fourth Lunar Science Conf., Geochim. Cosmochim. Acta, Suppl. 4*, **3**, 2803–2810.

Hartle, R. E., and Thomas, G. E.: 1974, *J. Geophys. Res.* **79**, 1519–1526.

Hirshberg, J., Asbridge, J. R., and Robbins, D. E.: 1972, *J. Geophys. Res.* **77**, 3583–3588.

Hodges, R. R.: 1973, *J. Geophys. Res.* **78**, 8055–8064.

Hodges, R. R.: 1974, *J. Geophys. Res.* **79**, 2881–2885.
Hodges, R. R. and Hoffman, J. H.: 1974a, *Proc. Fifth Lunar Science Conf., Geochim. Cosmochim. Acta, Suppl. 5*, **3**, 2955–2961.
Hodges, R. R., and Hoffman, J. H.: 1974b, *Geophys. Res. Letters* **1**, 69–71.
Hodges, R. R. and Johnson, F. S.: 1968, *J. Geophys. Res.* **73**, 7307–7317.
Hodges, R. R., Hoffman, J. H., and Johnson, F. S.: 1974, *Icarus*, **21**, 415–426.
Hoffman, J. H. and Hodges, R. R.: 1975, The Moon, **14**, 159–167.
Housley, R. M.: 1974, 'Ion Sputtering and Volatile Transport', paper presented at Conference on Origin and Evolution of the Lunar Regolith, Houston.
Johnson, F. S., Carroll, J. M., and Evans, D. E.: 1972, *Proc. Third Lunar Science Conf., Geochim. Cosmochim. Acta, Suppl. 3*, **3**, 2231–2242.
Kopal, Z.: 1966, *An Introduction to the Study of the Moon*, (Chapter 6), Gordon and Breach, New York.
Latham, G., Dorman, J., Duennebier, F., Ewing, M., Lammlein, D., and Nakamura, Y.: 1973, *Proc. Fourth Lunar Science Conf., Geochim. Cosmochim. Acta, Suppl. 4*, **3**, 2515–2528.
Manka, R. H. and Michel, F. C.: 1971, *Proc. Second Lunar Science Conf., Geochim. Cosmochim. Acta, Suppl. 2*, **2**, 1717–1728.
Taylor, S. R. and Jakeš, P.: 1974, *Proc. Fifth Lunar Science Conf., Geochim. Cosmochim. Acta, Suppl. 3*, **2**, 1287–1305.
Wilcox, J. M., Schatten, K. H., and Ness, N. F.: 1967, *J. Geophys. Res.* **72**, 19–26.